Supporting Information

Enrichment-Stowage-Cycle Strategy for Ultrasensitive Electrochemiluminescent Detection of HIV-DNA with Wide Dynamic Range

Zhen Wu, Fanwei Luo, Wei Wen*, Xiuhua Zhang, Shengfu Wang*

Hubei Collaborative Innovation Center for Advanced Organic Chemical Materials, Ministry of Education Key Laboratory for the Synthesis and Application of Organic Functional Molecules and College of Chemistry and Chemical Engineering, Hubei University, Wuhan 430062, China.

*Corresponding author: Wei Wen, Email: wenwei@hubu.edu.cn. Shengfu Wang, Email: wangsf@hubu.edu.cn.

Table of contents

S1. Preparation of carboxyl-functioned ENs.

The prepared ENs were washed with ethanol for 3 times and dispersed into 4 mL 20 g/L polyvinylpyrrolidone (PVP-k30) for 24 h with gentle shaking. Then 95 μL ammonium hydroxide and 125 μL ethanol containing 10% tetraethyl orthosilicate (TEOS) were added into the solution and continued the reaction until the surface potential of nanospheres reached −25 mV. Subsequently, 125 μL ethanol containing 10% (3-aminopropyl)triethoxysilane (APTES) was added and continued the reaction until the surface potential of nanospheres reached 25 mV. Then the nanospheres were centrifuged and washed with ethanol for 3 times and dispersed into 1 mL dimethylformamide (DMF) solution containing 8 g/L succinic anhydride for 3 h with gentle shaking. After washing with ethanol and ultrapure water, the precipitation was dispersed into 1 mL ultrapure water to obtain carboxyl-functioned ENs.

Table S1. Sequences of Oligonucleotides Used in This Assay

	Sequence (5'-3')
H1	NH_2-$(CH_2)_6$-ATGTGGA*AAATCTCTAGCAGT*CCATGTGTAGA *ACTGCTAGAGATTTT* [a, b]
H2	NH_2-$(CH_2)_6$-TAGCAGT*TCTACACATGG*ACTGCTAGAGATTT *CCATGTGTAGA* [a, b]
HIV-DNA	ACTGCTAGAGATTTTCCACAT [a]
1-base mismatch	ACTGCTAGAGATTTTCCATAT [c]
3-base mismatch	ACTGTTAGAGACTTTCCATAT [c]
HBV	ATACCACATCATCCATATAACTGAAAGCCA
HCV	ATCTCCAGGCATTGAGCGGGTTTATCCAGGA

[a] Sequences of the same color could complement with each other. [b] Sequences in italic represent complementary bases in one hairpin DNA. [c] Bases with underline are the differences with target.

S2. Optical properties of ENs.

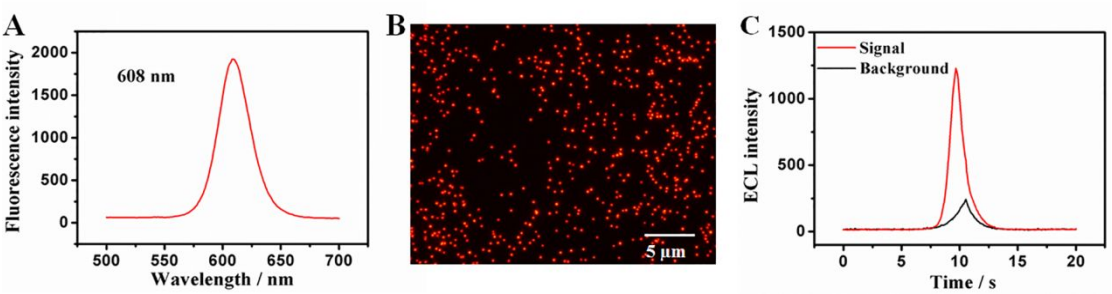

Figure S1. (A) Fluorescence spectrum of ENs. (B) Fluorescence image of ENs under a fluorescence inverted microscopy. (C) ECL spectra of ENs and background.

S3. Preparation and verification of H2-ENs.

Based on the layer-by-layer assembly method, a novel kind of ENs was prepared by assembling three layers of QDs on the surface of copolymer nanospheres. The surface of ENs was rich in carboxyl groups and its zeta potential was −31.4 mV. After modifying H2, some carboxyl groups on ENs surface were consumed and the zeta potential was changed to −25.3 mV.

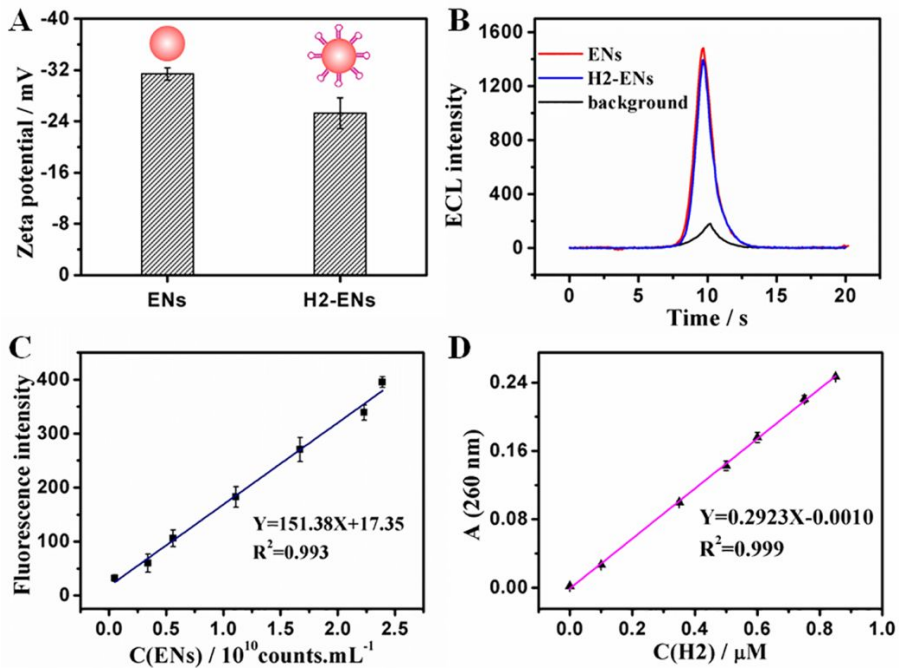

Figure S2. (A) Zeta potentials of ENs and H2-ENs. (B) ECL spectra of ENs, H2-ENs and background. (C) Linear curve between ENs concentrations and fluorescence intensities at 608 nm. (D) Linear curve between H2 concentrations and absorption intensities at 260 nm.

S4. Characterization of H1-MBs.

The surface of MBs was rich in carboxyl groups. Based on amide bond reaction, H1 was modified to the surface of MBs to fabricate capture probes and DLS was

applied to characterize the modification process. Thus, some carboxyl groups on MBs surface were consumed and the zeta potential of MBs changed from −27.8 mV to −17.3 mV (Figure S3A), indicating the successful preparation of H1-MBs.[1] In order to further investigate the number of H1 on each MBs, the curve between MBs concentrations and UV-vis absorption intensities at 600 nm, and the relationship between H1 concentrations and UV-vis absorption intensities at 260 nm were obtained (Figure S3B,C). According to the adsorption intensities of H1-MBs samples at 600 nm and 260 nm respectively, the number of H1 on each MBs was estimated to be about 1.4×10^3. With so many binding sites, H1-MBs could efficiently capture and separate HIV-DNA from complex samples.

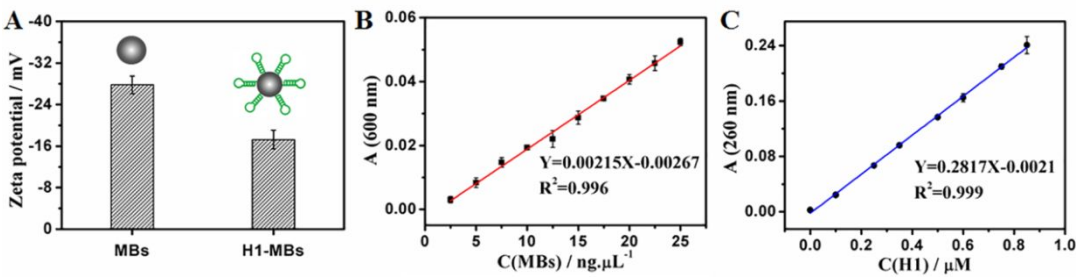

Figure S3. (A) Zeta potentials of MBs and H1-MBs. (B) Linear curve between MBs concentrations and UV-vis absorption intensities at 600 nm. (C) Linear curve between H2 concentrations and absorption intensities at 260 nm.

S5. Optimization of M-GCE.

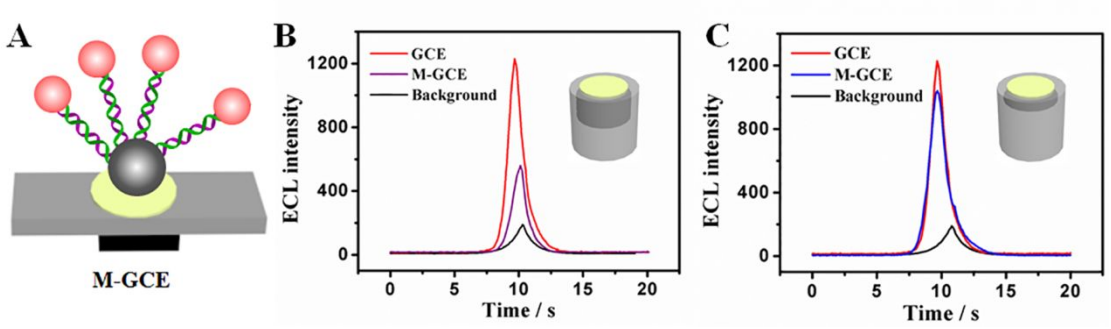

Figure S4. (A) Schematic diagram of the magnetic complexes captured onto the M-GCE surface. (B) ECL spectra between M-GCE with four pieces of magnets and GCE without magnet. (C) ECL spectra between M-GCE with one piece of magnet and GCE without magnet.

S6. Amplification of SDA.

The feasibility of SDA was characterized by polyacrylamide gel electrophoresis. As shown in Figure S5A, the generation of long dsDNA in the presence of HIV-DNA (lane 5) indicated the successful hybridization reaction between HIV-DNA and H1. With the addition of H2, the appearance of longer dsDNA (Lane 6) demonstrated the occurrence of SDA.[2] However, no long nucleic acids were appeared in the absence of HIV-DNA (Lane 7), indicating the feasibility and accuracy of SDA. H1 and H2 were designed to implement SDA and they were modified to MBs and ENs surface respectively to prepare H1-MBs and H2-ENs. It can be seen from the TEM image that some MBs were combined with several ENs (Figure S5B). The reason might be that each MB had multiple H1 molecules and the released target DNA by SDA reaction could be hybridized with unreacted H1 on the surface of MB.

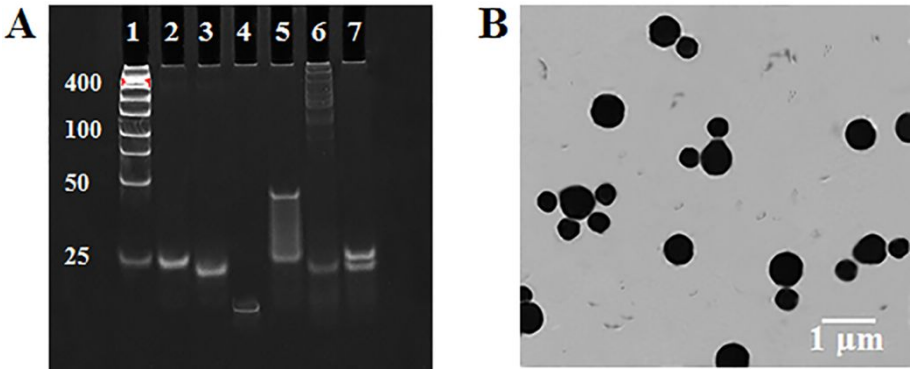

Figure S5. (A) Polyacrylamide gel electrophoresis analysis for SDA (15 % polyacrylamide, 120 V for 70 min). Lane 1: Marker, Lane 2: H1, Lane 3: H2, Lane 4: HIV-DNA, Lane 5: H1+HIV-DNA, Lane 6: H1+HIV-DNA+H2, Lane 7: H1+H2. (B) TEM image of H1-MBs/HIV-DNA/H2-ENs complexes.

Table S2. Summary of the Detection of HIV-DNA with Different Methods

method	label	linear range	detection limit	ref
Fluorescence polarization	ssDNA/graphene oxide	50-2000 pM	38.6 pM	42
Fluorescence	Mg^{2+}/DNAzyme	0.1 pM-1 nM	61 fM	43
Visual biosensor	glucose oxidase	0.01-120 nM	4.8 pM	7
Electrochemistry	$[Ru(NH_3)_6]^{3+}$	0.1 pM-10 nM	150 fM	9
Fluorescent LFA strip	CdTe QDs	1 pM-10 nM	0.76 pM	23
ECL	ENs	0.05 pM-50 nM	39.81 fM	this work

S7. Stability of ECL Signals.

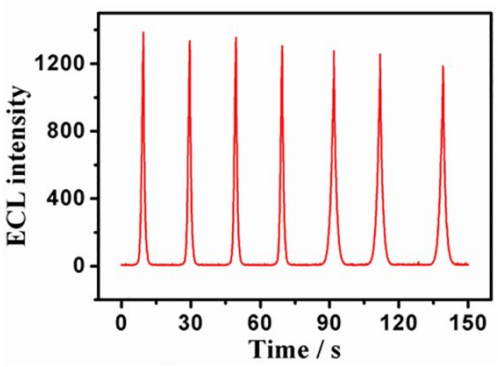

Figure S6. ECL spectrum under continuous scan.

Table S3. Recovery Rate of the Method in Complex Samples

Sample	Added (nM)	Found (nM)	Recovery (%)	RSD (%)
Milk	0.15	0.1479	98.60	6.306
Urine	0.15	0.1578	105.2	6.747
FBS	0.15	0.1585	105.7	12.29
Whole Blood	0.15	0.1357	90.47	13.53

Reference

(1) Chen, L.; Wu, L. L.; Zhang, Z. L.; Hu, J.; Tang, M.; Qi, C. B.; Li, N.; Pang, D. W. Biofunctionalized magnetic nanospheres-based cell sorting strategy for efficient isolation, detection and subtype analyses of heterogeneous circulating hepatocellular carcinoma cells. *Biosens. Bioelectron*. **2016**, *85*, 633–640.

(2) Guo, W. J.; Wu, Z.; Yang, X. Y.; Pang, D. W.; Zhang, Z. L. Ultrasensitive electrochemical detection of microRNA-21 with wide linear dynamic range based on dual signal amplification. *Biosens. Bioelectron*. **2019**, *131*, 267–273.